

# Cost-time trade-off in diffusion with stochastic return: optimal resetting potential and Pareto front

**Prashant Singh**

Niels Bohr International Academy, Niels Bohr Institute, University of Copenhagen,  
Blegdamsvej 17, 2100 Copenhagen, Denmark

E-mail: prashant.singh@nbi.ku.dk

**Abstract.** Resetting processes, where a system is regularly returned to a given state after a fixed or random duration, offer a simple strategy to generate non-equilibrium properties and optimize search operations. While earlier theoretical frameworks focused on instantaneous resetting, wherein the system is directly teleported to a resetting state, there is a growing interest in physical resetting mechanisms that involve a finite return time. In this paper, we present an exact thermodynamic analysis of a diffusing particle whose position is intermittently reset to a specific site by employing a stochastic return protocol with external confining trap. We derive a renewal formula for the joint distribution of the first-passage time and the work done in terms of the characteristic measures of the underlying process. Using this formula, we compute general expressions for the averages of the work done and the first-passage time for an arbitrary confining potential. We next focus on a family of potentials  $U_R(x) \sim |x|^m$  with  $m > 0$ , and optimise, with respect to the potential shape, the expected first-passage time for a given value of the work done. The Pareto front associated with this optimisation is exactly obtained, along with the optimal resetting potentials. Finally, we use this to demonstrate a trade-off relation between the first-passage time and the work done.

## 1. Introduction

Over the past decade, stochastic resetting has become a widely studied topic in statistical physics. Resetting processes, in which a system is regularly returned to a given state after a fixed or random duration, offer a simple strategy to generate non-equilibrium properties and optimize search operations [1–4]. The subject has garnered significant interest across cross-disciplinary disciplines including physics [3–17], chemical and biological processes [18–21], income models [22, 23] and computer science [24, 25]. Earlier theoretical frameworks mostly focused on instantaneous resetting, wherein the system is directly teleported to a resetting state. A commonly studied model is that of a diffusing particle whose position  $x(t)$  resets to a value  $x_R$  at a rate  $r$ . In a small time

interval  $[t, t + \Delta t]$ , the position evolves as

$$x(t + \Delta t) = x(t) + \Delta t \eta(t), \quad \text{with probability } (1 - r\Delta t), \quad (1)$$

$$= x_R, \quad \text{with probability } r\Delta t, \quad (2)$$

where  $\eta(t)$  is the Gaussian white noise with zero mean and correlation  $\langle \eta(t)\eta(t') \rangle = 2D\delta(t - t')$ . During resetting, the position instantaneously changes its value to  $x_R$ . Several theoretical results have been already established for this model as well as for other models in the past one decade [26]. For example, this simple strategy gives a finite average first-passage time in models which otherwise have infinite average first-passage time. We refer to [26–30] and references therein for a thorough review on the topic. While these studies provide useful insights in understanding the ramifications of resetting, they fail to capture the intricacies of real models where resetting is usually non-instantaneous. Single-particle experiments on resetting often involve non-zero return times [31–33]. This has naturally prompted some recent attempts to account for the time penalty occurring during non-instantaneous resetting events [20, 34–46]. Some works, for instance, incorporate a residence time following each resetting event [40–42], while others involve intermittently switching on and off certain confining potentials [45, 46].

Stochastic return dynamics is a useful extension of the latter strategy [47–50]. In this case, a particle evolves under its natural dynamics. However, one intermittently switches on a confining trap that takes the particle to a desired location. Upon reaching this location, the trap is switched off, and the particle resumes its natural dynamics. Such a protocol also gives rise to a finite and optimised value of the mean first-passage time, in contrast to its diverging value for the simple diffusion [47, 48]. However, it is more realistic since the particle takes a non-zero time to reach the resetting location.

Employing the confining potential incurs an energetic cost [51]. Several works have also focused on the thermodynamic aspects of resetting [52–64]. According to the framework of stochastic thermodynamics, any temporal change of the external trap is related to the work done on the system [65, 66]. Hence, it is quite natural to anticipate that thermodynamics will play a crucial role in the stochastic return models. How does thermodynamics impact the search strategies in these models? Despite of paramount importance, the number of exactly solvable thermodynamically efficient search problems with non-instantaneous resetting seems very limited [63]. There are, to the best of our knowledge, no results on what confining potential optimises the search time while keeping the thermodynamic cost function fixed to a value. Can one construct Pareto front for such an optimisation problem [67]? This paper aims to partially fill this gap.

In this paper, we construct a comprehensive path decomposition methodology to study the work done and the first-passage time for diffusion with stochastic returns. Our approach yields the the exact joint distribution of the these two quantities completely in terms of the characteristic measures of the underlying process. Using this formula, we derive general expressions for the averages of the work done and the first-passage time for any arbitrary confining potential. We next focus on a family of potentials  $U_R(x) \sim |x|^m$  with  $m > 0$ , and optimise, with respect to the potential shape, the expected first-passage

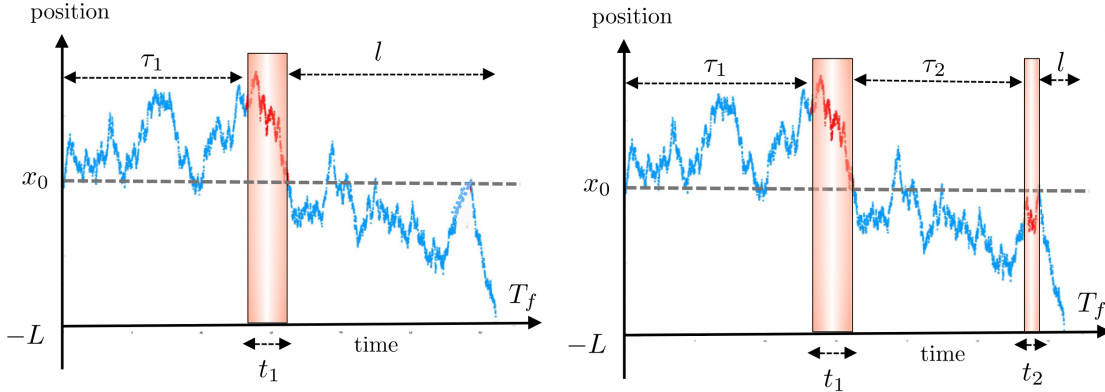


**Figure 1.** Schematic illustration of a trajectory of a stochastic process undergoing one (left panel) and two (right panel) resetting events at a rate  $r$ . The resetting events, shown in red within the shaded regions, are implemented using a trapping potential  $U_R(x)$  with its minimum located at the origin  $x_0 = 0$ . During these events, the particle makes first-passage visits to the origin, with the associated first-passage times denoted by  $t_1, t_2, \dots, t_n$  (with  $n = 1$  for the left panel and  $n = 2$  for the right panel). Apart from this, the particle follows its original dynamics (shown in blue) for durations  $\tau_1, \tau_2, \dots, \tau_n$ , each drawn from the exponential distribution  $\rho(\tau) = re^{-r\tau}$ . The global first-passage time to the position  $x = -L$  (with  $L > 0$ ) is denoted by  $T_f$ .

time for a given fixed value of the work. Using the optimal solutions for different values of the work, we construct the exact Pareto front, and use it to demonstrate a trade-off relation between the first-passage time and the work done. Our work offers some perspective on the design and control of cost efficient search mechanisms.

The remainder of paper is structured as follows: in section (2), we introduce our model and fix all notations relevant for the subsequent study. Section (3) presents the derivation of the renewal formula for the joint distribution, which becomes instrumental in deriving the mean work in section (4) and the mean first-passage time in section (5) for arbitrary resetting potentials. Section (6) discusses Pareto optimisation and the trade-off relation, followed by the conclusion in section (7).

## 2. Model

Let us consider a freely diffusing particle in one dimension whose position at time  $t$  is represented by a continuous variable  $x(t)$ . The process is governed by the overdamped law of motion

$$\frac{dx}{dt} = \eta(t), \quad (3)$$

where  $\eta(t)$  is the Gaussian white noise with zero mean and correlation  $\langle \eta(t)\eta(t') \rangle = 2D\delta(t - t')$ . Here  $D$  is the diffusion coefficient which will be set to  $1/2$  throughout this paper. We also fix the initial position to the origin,  $x_0 = 0$ . The particle evolving with this dynamics also experiences resetting at a constant rate  $r$ . During the resetting event,

an external confining potential  $U_R(x)$  is switched on such that the particle is facilitated to move towards the minima of this potential. We assume that this minima is unique and located at the origin. During the return phase, the position evolves according to

$$\frac{dx}{dt} = -\frac{\partial U_R(x)}{\partial x} + \eta(t). \quad (4)$$

It ends whenever the particle reaches the origin for the first time, at which point the potential is switched off. After this, it again evolves according to Eq. (3) until the next resetting event. Thus, the process evolves in a series of diffusive and resetting phases, and it can be succinctly written as

$$\frac{dx}{dt} = -\frac{\partial V(x, \Lambda(t))}{\partial x} + \eta(t), \quad \text{with } V(x, \Lambda(t)) \equiv \Lambda(t)U_R(x). \quad (5)$$

Here  $\Lambda(t)$  is a random dichotomous variable which takes value 1 if the particle is in the return phase and 0 if it is in the diffusive phase. Notice that for any finite  $U_R(x)$ , the return phase is non-instantaneous and the particle spends a non-zero time to reach the resetting site. The process (5) is repeated until the particle reaches the target position located at  $x(t) = -L$  (with  $L > 0$ ) for the first time in the diffusive phase. We denote this global first-passage time by  $T_f$ , see Figure 1.

While implementing resetting using trapping potentials, one always incurs some thermodynamic cost, i.e. work [51, 63]. In the last few decades, the framework of stochastic thermodynamics has been rigorously developed and this has allowed us to identify thermodynamic quantities for stochastic systems such as in Eq. (5) [65, 66]. The total stochastic work involved in implementing the resetting until the first-passage time  $T_f(L)$  is given by

$$W(L) = \int_0^{T_f} dt \dot{\Lambda}(t) \frac{\partial V(x, \Lambda(t))}{\partial \Lambda(t)} = \int_0^{T_f} dt \dot{\Lambda}(t) U_R(x(t)). \quad (6)$$

We are interested in calculating the statistical properties of this cost for a general potential  $U_R(x)$ . To achieve this, we will construct a renewal formula for the joint distribution of the work done and the global first-passage time in terms of the characteristic properties of the underlying processes in Eqs. (3) and (4). Using this formula, we derive general expressions for the averages of the work done and the first-passage time for any arbitrary confining potential. This will be instrumental in (i) demonstrating a trade-off relation between these two quantities including calculating the Pareto front, and (ii) finding optimal resetting potentials for a thermodynamically efficient search in a class of potentials.

It is important to note that our first-passage event  $T_f$  is achieved only during the diffusive phase, and not during the return phase. While this is valid for strongly confining potentials, it will break down if the potential is only weakly confining and  $L$  is not large. Here we still adopt this crucial assumption since our primary goal is to construct the methodology to study the cost-time relation. This simplification allows us

to derive precise and elegant expressions, and compare them directly with simulations. It also enables us to provide a thermodynamic interpretation of some non-thermodynamic cost functions studied for resetting systems. Modifying our framework to relax this assumption is possible, but it makes the problem analytically less tractable. We aim to address this in a future work.

### 3. Renewal formula for the joint distribution of $W(L)$ and $T_f(L)$

We first look at the joint distribution  $\mathcal{P}(W, T_f)$  of the work  $W(L)$  and the first-passage time  $T_f(L)$  in presence of resetting.

#### 3.1. Number of resetting $n = 1$

To begin with, consider the situation where particle experiences only one resetting event ( $n = 1$ ) before it gets absorbed at  $x = -L$ . An schematic illustration of such a trajectory is shown in Figure 1 (left panel). Let us break this trajectory in three parts: (i) pre-reset part  $[0, \tau_1]$ , (ii) reset part  $[\tau_1, \tau_1 + t_1]$  and (iii) post-reset part  $[\tau_1 + t_1, \tau_1 + t_1 + l]$ . In the pre-reset part, the particle, starting from the origin, reaches some position  $x(\tau_1) = x_1$  at time  $\tau_1$ . Moreover, the particle always stays above the target at  $-L$ . Therefore, the statistical weight of this part of the trajectory is just the propagator  $P_0(x_1, \tau_1; -L)$  of a freely diffusing particle with an absorbing wall located at  $x = -L$ .

We next examine the reset part. In this phase, the particle begins its motion from  $x_1$  and makes a first-passage visit to the origin in duration  $t_1$ . Therefore, the contribution from this segment is the distribution  $F_R(t_1 | x_1; 0)$  of the first-passage time  $t_1$  to the origin, given that the particle was at  $x_1$  at the start of this segment. The subscript ‘ $R$ ’ in  $F_R(t_1 | x_1; 0)$  is used to indicate that this first-passage time is measured for model (4) with resetting potential  $U_R(x)$ . Finally, we investigate the post-resetting part in Figure 1 (left panel). As clear from this figure, the particle, beginning from the origin, makes a first-passage visit at time  $l$  to the target location at  $x = -L$ . Then, the contribution from this part is also the first-passage distribution  $F_0(l | 0; -L)$  for the diffusion (with no resetting potential).

Since the process is a Markov process for all three segments, the total path weight of the entire trajectory is equal to the product of these three contributions. Hence, we have

$$\text{Path weight} \Big|_{n=1} = P_0(x_1, \tau_1; -L) \rho(\tau_1) F_R(t_1 | x_1; 0) F_0(l | 0; -L) e^{-r\tau_1}. \quad (7)$$

We have weighted  $P_0(x_1, \tau_1; -L)$  by the resetting time distribution  $\rho(\tau_1) = r e^{-r\tau_1}$ . Moreover, in the post-resetting phase, the particle does not experience any resetting event till time  $l$ , the probability of which is  $e^{-rl}$ . This results in  $e^{-rl}$  factor accompanying the last term.

Once the path weight is calculated, we need to supplement it with the correct values of the work and the first-passage time. Calculating  $T_f$  is straightforward since it is given

by the sum of all times appearing above, i.e.,  $T_f = \tau_1 + t_1 + l$ . On the other, for work, we need to specify  $\Lambda(t)$  in Eq. (6). Recall that  $\Lambda(t)$  is a dichotomous variable which takes value 1 if the particle is in the return phase and 0 if it is in the diffusive phase. Looking at Figure 1, we can write it as [51]

$$\Lambda(t) = \Theta(t - \tau_1) - \Theta(t - \tau_1 - t_1), \quad (8)$$

where  $\Theta(t - \tau_1)$  stands for the Heaviside theta function. It takes value 1 if  $t > \tau_1$  and 0 otherwise. Taking the derivative of  $\Lambda(t)$  and plugging it in Eq. (6), we obtain  $W = U(x(\tau_1)) - U(x(\tau_1 + t_1))$ . Noting that, at the end of any resetting phase, the particle is at the origin, we get  $x(\tau_1 + t_1) = 0$ . Furthermore, the trapping potential  $U_R(x)$  has its minimum value located at the origin. Without any loss of generality, we take this minimum value to be zero,  $U(x(\tau_1 + t_1)) = 0$ . The stochastic work then becomes

$$W = U_R(x_1). \quad (9)$$

Combining this with Eq. (7), we finally obtain the contribution of  $n = 1$  events to the joint distribution  $\mathcal{P}(W, T_f)$  as

$$\begin{aligned} \mathcal{C}_1 = \int_{-L}^{\infty} dx_1 \int_0^{\infty} d\tau_1 \int_0^{\infty} dt_1 \int_0^{\infty} dl & P_0(x_1, \tau_1; -L) \rho(\tau_1) F_R(t_1 | x_1; 0) F_0(l|0; -L) e^{-rl} \\ & \times \delta(T_f - \tau_1 - t_1 - l) \delta(W - U_R(x_1)). \end{aligned} \quad (10)$$

The delta functions enforce the correct values of work and first-passage time.

### 3.2. Number of resetting $n = 2$

We next calculate the contribution of those events with  $n = 2$ . A schematic illustration of this is shown in Figure 1 (right panel). For this case, we break the trajectory into five parts: (i) pre-first reset part  $[0, \tau_1]$ , (ii) first reset part  $[\tau_1, \tau_1 + t_1]$ , (iii) pre-second reset part  $[\tau_1 + t_1, \tau_1 + t_1 + \tau_2]$ , (iv) second reset part  $[\tau_1 + t_1 + \tau_2, \tau_1 + t_1 + \tau_2 + t_2]$ , and (v) post-second reset part  $[\tau_1 + t_1 + \tau_2 + t_2, \tau_1 + t_1 + \tau_2 + t_2 + l]$ . For each of these segments, we can calculate the statistical weight using the same physical rationale as before. For example, in segment (i), the particle, starting from the origin, reaches some position  $x(\tau_1) = x_1$  at time  $\tau_1$  in presence of an absorbing wall at  $x = -L$ . Contribution of this segment is  $P_0(x_1, \tau_1; -L)\rho(\tau_1)$ . Similarly, in segment (iii), the process remains above  $x = -L$  and reaches the position  $x(\tau_1 + t_1 + \tau_2) = x_1$  given that it started from the origin at the beginning of this segment. This again yields the contribution  $P_0(x_2, \tau_2; -L)\rho(\tau_2)$ . On the other hand, in segments (ii) and (iv), the particle makes first-passage visits to the origin at durations  $t_1$  and  $t_2$  starting from  $x_1$  and  $x_2$  respectively. We have  $F_R(t_1 | x_1; 0)$  and  $F_R(t_2 | x_2; 0)$  from these parts. Finally, in segment (v), the particle, during the free diffusive phase, reaches the target site  $x = -L$  in a time duration  $l$  without experiencing any resetting. The weight of this segment is  $F_0(l|0; -L)e^{-rl}$ .

Using Markovianity of the process, the total path probability then turns out to be

$$\text{Path weight} \Big|_{n=2} = P_0(x_1, \tau_1; -L) \rho(\tau_1) F_R(t_1 | x_1; 0) P_0(x_2, \tau_2; -L) \rho(\tau_2) \\ F_R(t_2 | x_2; 0) F_0(l|0; -L) e^{-rl}. \quad (11)$$

Furthermore, we have

$$\Lambda(t) = \Theta(t - \tau_1) - \Theta(t - \tau_1 - t_1) + \Theta(t - \tau_1 - t_1 - \tau_2) - \Theta(t - \tau_1 - t_1 - \tau_2 - t_2), \quad (12)$$

using which in Eq. (6) gives us the value of work

$$W = U_R(x_1) + U_R(x_2). \quad (13)$$

By incorporating this with Eq. (11), we ultimately derive the contribution of  $n = 2$  events to the joint distribution  $\mathcal{P}(W, T_f)$  as

$$\mathcal{C}_2 = \int_{-L}^{\infty} dx_1 \int_{-L}^{\infty} dx_2 \int_0^{\infty} d\tau_1 \int_0^{\infty} dt_1 \int_0^{\infty} d\tau_2 \int_0^{\infty} dt_2 \int_0^{\infty} dl P_0(x_1, \tau_1; -L) \rho(\tau_1) \\ \times F_R(t_1 | x_1; 0) P_0(x_2, \tau_2; -L) \rho(\tau_2) F_R(t_2 | x_2; 0) F_0(l|0; -L) e^{-rl} \\ \times \delta(T_f - \tau_1 - t_1 - \tau_2 - t_2 - l) \delta(W - U_R(x_1) - U_R(x_2)). \quad (14)$$

Proceeding similarly, one can write the contributions  $\mathcal{C}_3, \mathcal{C}_4, \dots$  to the joint distribution due to  $n = 3, 4, \dots$  number of resetting events. In particular, for the general value of  $n \geq 1$ , one gets

$$\mathcal{C}_n = \int_0^{\infty} dl \left[ \prod_{i=1}^n \int_{-L}^{\infty} dx_i \int_0^{\infty} d\tau_i \int_0^{\infty} dt_i P_0(x_i, \tau_i; -L) \rho(\tau_i) F_R(t_i | x_i; 0) \right] \\ \times F_0(l|0; -L) e^{-rl} \delta\left(T_f - l - \sum_{j=1}^n (\tau_j + t_j)\right) \delta\left(W - \sum_{j=1}^n U_R(x_j)\right), \quad (15)$$

whereas for  $n = 0$ , where no resetting occurs, one has

$$\mathcal{C}_0 = F_0(T_f|0; -L) e^{-rT_f} \delta(W). \quad (16)$$

Since the external potential is not switched on, the value of work for this case is equal to zero.

### 3.3. Joint distribution $\mathcal{P}(W, T_f)$

We now have all contributions essential for computing  $\mathcal{P}(W, T_f)$ . Summing all of them

$$\mathcal{P}(W, T_f) = \mathcal{C}_0 + \sum_{n=1}^{\infty} \mathcal{C}_n. \quad (17)$$

Each of these contributions involves delta function over both  $T_f$  and  $W$ . To get rid of them, it is useful to take Laplace transformations with respect to  $T_f$  ( $\rightarrow s$ ) and  $W$  ( $\rightarrow k$ ). Exploiting the convolution structure of  $\mathcal{C}_n$  in Eq. (15), its Laplace transform takes on a simple form

$$\text{Laplace Transform } \mathcal{C}_n = \bar{F}_0(s+r|0;-L) \left[ r \int_{-L}^{\infty} dx e^{-kU_R(x)} \bar{P}_0(x, s+r; -L) \bar{F}_R(s|x;0) \right]^n,$$

where  $\bar{F}_0(s|0;-L)$ ,  $\bar{F}_R(s|x;0)$  and  $\bar{P}_0(x, s; -L)$  are respectively the Laplace transforms of  $F_0(t|0;-L)$ ,  $F_R(t|x;0)$  and  $P_0(x, t; -L)$ . Utilizing this on Eq. (17) and performing the summation over  $n$  yields

$$\mathcal{Z}(k, s) = \frac{\bar{F}_0(s+r|0;-L)}{1 - r \int_{-L}^{\infty} dx e^{-kU_R(x)} \bar{P}_0(x, s+r; -L) \bar{F}_R(s|x;0)}, \quad (18)$$

where  $\mathcal{Z}(k, s)$  denotes the double Laplace transformation of  $\mathcal{P}(W, T_f)$ . Eq. (18) is the first main result of our paper. This renewal formula gives the exact joint distribution in terms of the underlying propagators and the first-passage properties.

Our formula also gives the correct normalisation. To see this, we put  $k = 0$  and  $s = 0$  in Eq. (18). We also use the normalisation property of the distribution  $\bar{F}_R(s=0|x;0) = 1$ . One then has

$$\mathcal{Z}(k=0, s=0) = \frac{\bar{F}_0(r|0;-L)}{1 - r \int_{-L}^{\infty} dx \bar{P}_0(x, r; -L)}. \quad (19)$$

We next identify that the integration  $\int_{-L}^{\infty} dx P_0(x, t; -L)$  simply represents the probability  $Q_0(t; -L)$  that the particle, starting from the origin, has survived the absorbing wall at  $x = -L$ . The corresponding first-passage distribution is expressed as the first derivative of the survival probability  $F_0(t|0; -L) = -dQ_0(t; -L)/dt$ . In terms of the Laplace variable, these relations translate to

$$\int_{-L}^{\infty} dx \bar{P}_0(x, s; -L) = \bar{Q}_0(s; -L), \text{ and } \bar{F}_0(s|0; -L) = 1 - s\bar{Q}_0(s; -L). \quad (20)$$

Substituting them in Eq. (19), we obtain the correct normalisation  $\mathcal{Z}(k=0, s=0) = 1$ . This further validates our renewal formula. In what follows, we will use this formula to study the statistics of  $W$  and  $T_f$  for a general resetting potential.

#### 4. Work for a general resetting potential

We will first use Eq. (18) to analyze the statistics of work. Setting  $s = 0$  and applying the normalization  $\bar{F}_R(s=0|x;0) = 1$  gives us the generating function of  $W(L)$  as

$$\mathcal{Z}(k, s=0) = \frac{\bar{F}_0(r|0;-L)}{1 - r \int_{-L}^{\infty} dx e^{-kU_R(x)} \bar{P}_0(x, r; -L)}. \quad (21)$$



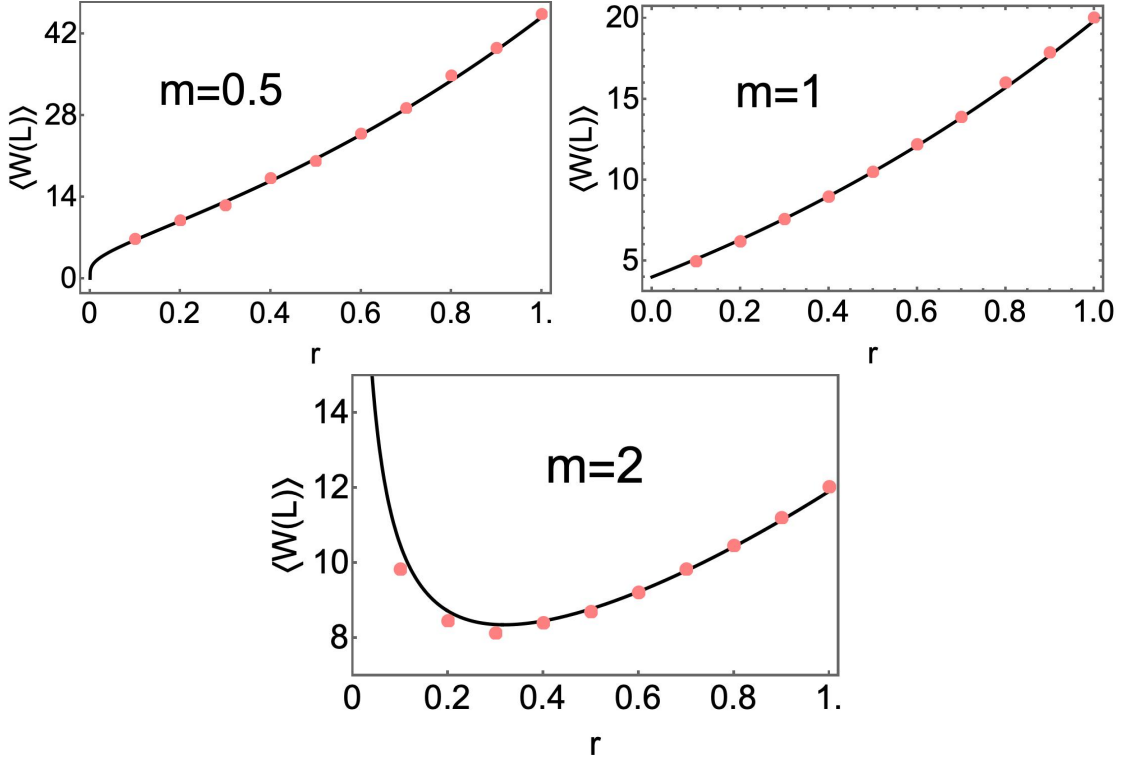


**Figure 2.** Numerical verification of the mean thermodynamic work for a class of resetting potentials  $U_R(x) = \alpha|x|^m/m$ . For all three panels, solid lines represent the analytic formula in Eq. (26) while symbols are the simulation data. Parameters used for the comparison are  $L = 2$ ,  $\alpha = 2$ .

Interestingly, our expression matches with the renewal equation for some other non-thermodynamic cost functions studied in the context of instantaneous resetting processes [68, 69]. In such a set-up, the particle undergoes instantaneous resetting from some position  $x'$  to the origin. If one defines  $U_R(x')$  as the cost for each resetting event, then the renewal formula for this cost till its first-passage time is exactly the same as Eq. (21). If we integrate out the return time in our problem and focus only on the work done, it becomes mathematically equivalent to [68, 69]. However, the first-passage time properties will be different, as we show below. We especially emphasize that these works deal with idealized instantaneous resetting, while our derivation is for non-instantaneous resetting implemented through external confining traps.

Taking derivative of  $\mathcal{Z}(k, s = 0)$  with  $k$  and then setting  $k = 0$ , we obtain the mean value of work as

$$\langle W(L) \rangle = \frac{r}{\bar{F}_0(r | 0; -L)} \int_{-L}^{\infty} dx U_R(x) \bar{P}_0(x, r; -L). \quad (22)$$

This expression is valid across any confining potential  $U_R(x)$ . For a family of potentials

$$U_R(x) = \frac{\alpha}{m}|x|^m, \quad \text{with } m > 0, \alpha > 0, \quad (23)$$

along with the Brownian motion results [70]

$$\bar{F}_0(s | 0; -L) = e^{-\sqrt{2s}L}, \quad (24)$$

$$\bar{P}_0(x, s; -L) = \frac{1}{\sqrt{2s}} \left[ e^{-\sqrt{2s}|x|} - e^{-\sqrt{2s}(x+2L)} \right], \quad (25)$$

the integration over  $x$  in Eq. (22) can be analytically carried out. The mean work  $\langle W(L) \rangle$  is then given by

$$\begin{aligned} \langle W(L) \rangle = & \frac{\alpha}{2m(2r)^{m/2}} \left[ \Gamma(m+1) \left\{ 2 \sinh(\sqrt{2r}L) + e^{\sqrt{2r}L} - (-1)^{-m-1} e^{-\sqrt{2r}L} \right\} \right. \\ & \left. + (-1)^{-m-1} e^{-\sqrt{2r}L} \Gamma(m+1, -\sqrt{2r}L) - e^{\sqrt{2r}L} \Gamma(m+1, \sqrt{2r}L) \right], \quad (26) \end{aligned}$$

where  $\Gamma(m, y)$  is the upper incomplete Gamma function. For the linear case ( $m = 1$ ), same expression was obtained using the Feynman–Kac method [63]. Our method goes beyond the linear case and gives  $\langle W(L) \rangle$  for a general resetting potential  $U_R(x)$ . In Figure 2, we have compared our theoretical result with the numerical simulation for three different values of  $m$ . We find a good agreement between theory and simulation for all three cases.

From this figure, we also see that one gets different behaviours of the mean as  $r \rightarrow 0^+$ . While for  $m > 1$ ,  $\langle W(L) \rangle$  diverges as  $r \rightarrow 0^+$ , it approaches zero for  $m < 1$ . For the marginal case  $m = 1$ ,  $\langle W(L) \rangle$  takes a constant non-zero value. This was also observed generically in [68] and in [63] for the  $m = 1$  case. For small values of  $r$ , the particle experiences a small number of resets. Therefore, the joint distribution  $\mathcal{P}(W, T_f)$  in Eq. (17) will have leading contributions from  $\mathcal{C}_n$  with small  $n$ . Notice that  $\mathcal{C}_0$  in Eq. (16) includes a delta function term  $\delta(W)$ , which results in zero contribution to  $\langle W(L) \rangle$ . This indicates that the first non-zero contribution to  $\langle W(L) \rangle$  will come from  $\mathcal{C}_1$  in Eq. (14). In Appendix A, we show this contribution is equal to

$$\langle W(L) \rangle \simeq \frac{\alpha L \Gamma(m+1)}{m} (2r)^{\frac{1-m}{2}} \quad \text{as } r \rightarrow 0^+. \quad (27)$$

It clearly demonstrates that the mean value diverges as  $r^{(1-m)/2}$  for  $m > 1$  whereas it converges to zero for  $m < 1$ . For  $m = 1$ , it possesses a non-zero value of  $\alpha L$  independent of the resetting rate  $r$ .

## 5. First-passage time for a general resetting potential

In this section, we will present results on the global first-passage time. For this, we set  $k = 0$  in our renewal formula in Eq. (18).

$$\mathcal{Z}(k = 0, s) = \frac{\bar{F}_0(s+r | 0; -L)}{1 - r \int_{-L}^{\infty} dx \bar{P}_0(x, s+r; -L) \bar{F}_R(s | x; 0)}. \quad (28)$$

Although the renewal formula for work in Eq. (21) is mathematically equivalent to the instantaneous reset case [68], the renewal formulas for first-passage time are different.

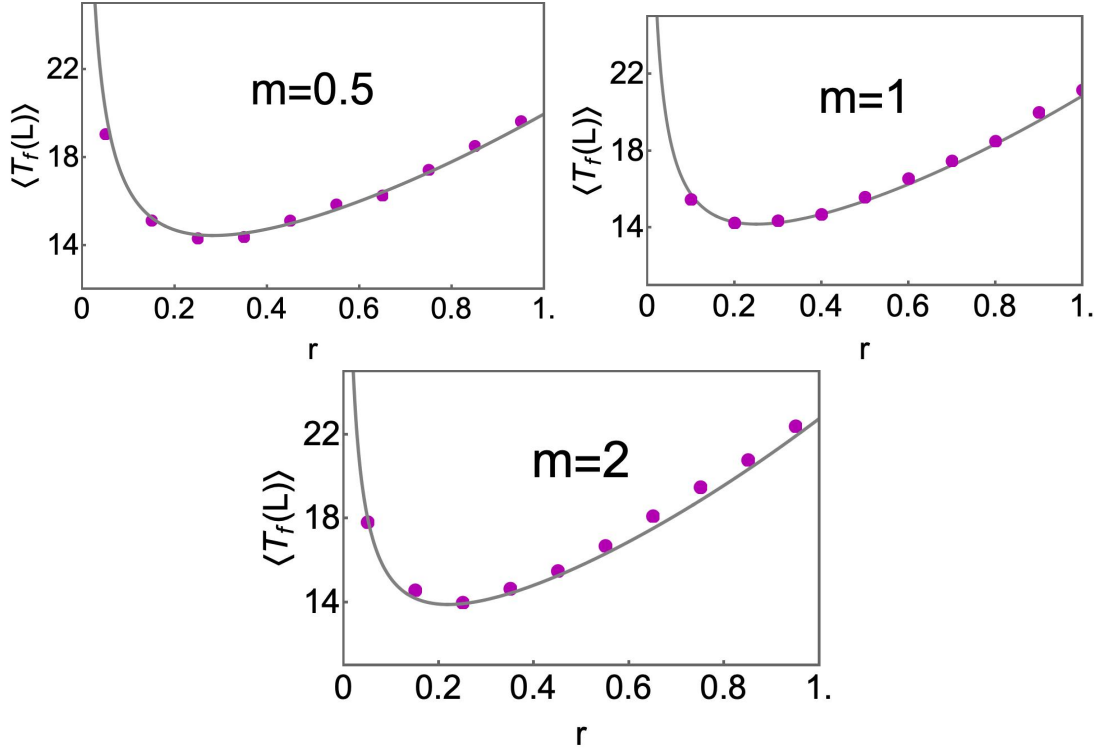


**Figure 3.** Comparison of the mean first-passage time  $\langle T_f(L) \rangle$  with the numerical simulations for the resetting potential  $U_R(x) = \alpha|x|^m/m$ . In all panels, solid lines represent the theoretical formula while symbols are the simulation data. The theoretical expressions are given in Eq. (33) for  $m = 1$ , in Eq. (34) for  $m = 1/2$  and in Eq. (29) for  $m = 2$ . Parameters used are  $L = 2$ ,  $\alpha = 2$ .

Once again, we are interested in the mean  $\langle T_f(L) \rangle$ , for which we take the first derivative of  $\mathcal{Z}(k = 0, s)$  with  $s$  and then set  $s = 0$ . This gives

$$\langle T_f(L) \rangle = \frac{\bar{Q}_0(r; -L)}{\bar{F}_0(r | 0; -L)} + \frac{r}{\bar{F}_0(r | 0; -L)} \int_{-L}^{\infty} dx \bar{P}_0(x, r; -L) \langle t_f(x; 0) \rangle_R. \quad (29)$$

Here  $\langle t_f(x; 0) \rangle_R$  is the mean-first passage time to reach the origin starting from a position  $x$  following the resetting dynamics in Eq. (4). It is mathematically defined as

$$\langle t_f(x; 0) \rangle_R \equiv - \left. \frac{d\bar{F}_R(s | x; 0)}{ds} \right|_{s=0}. \quad (30)$$

Eq. (29) has an interesting physical interpretation. The first term  $\bar{Q}_0(r; -L)/\bar{F}_0(r | 0; -L) = (e^{\sqrt{2r}L} - 1)/r$  represents the mean-first passage time for a Brownian particle subjected to an instantaneous resetting at a rate  $r$  [1, 2]. However, for non-instantaneous resetting, the particle spends a non-zero amount of time during its return phase. The second term in Eq. (29) essentially amounts to this time. Our method gives its expression for a general potential. When  $U_R(x) \rightarrow \infty$ , then  $\langle t_f(x; 0) \rangle_R \rightarrow 0$  and our formula then reduces to the result of instantaneous resetting.

For a general potential  $U_R(x)$ , the mean first-passage time can be calculated to be [70]

$$\langle t_f(x; 0) \rangle_R = \begin{cases} 2 \int_x^0 dy e^{2U_R(y)} \int_{-\infty}^y dz e^{-2U_R(z)}, & \text{if } x < 0, \\ 2 \int_0^x dy e^{2U_R(y)} \int_y^{\infty} dz e^{-2U_R(z)}, & \text{if } x \geq 0. \end{cases} \quad (31)$$

For completeness, we have recalled this derivation in Appendix B. Eqs. (29) and (31) give us the mean first-passage time  $\langle T_f(L) \rangle$  for a general resetting potential. For the type of potentials in Eq. (23), we can obtain a closed analytic expression of  $\langle t_f(x; 0) \rangle_R$  as

$$\begin{aligned} \langle t_f(x; 0) \rangle_R &= \frac{2}{m} \left( \frac{m}{2\alpha} \right)^{\frac{1}{m}} \left[ \frac{(-1)^{-\frac{1}{m}}}{m} \left( \frac{m}{2\alpha} \right)^{\frac{1}{m}} \Gamma\left(\frac{1}{m}\right) \left\{ \Gamma\left(\frac{1}{m}\right) - \Gamma\left(\frac{1}{m}, -\frac{2\alpha}{m}|x|^m\right) \right\} \right. \\ &\quad \left. - \frac{m|x|}{2} \left( \frac{2\alpha|x|^m}{m} \right)^{\frac{1}{m}} {}_2F_2\left(\left\{1, \frac{2}{m}\right\}, \left\{1 + \frac{1}{m}, 1 + \frac{2}{m}\right\}; \frac{2\alpha}{m}|x|^m\right) \right], \end{aligned} \quad (32)$$

with  ${}_2F_2$  denoting the generalised hypergeometric function [see Appendix B.1 for derivation]. Substituting this expression in Eq (29), we have been able to analytically carry out the integration only for some values of  $m$ . For example for the case of linear potential  $m = 1$ , we obtain [63]

$$\langle T_f(L) \rangle = \frac{1}{r} \left( e^{\sqrt{2r}L} - 1 \right) + \frac{1}{\alpha\sqrt{2r}} \left[ 2 \sinh(\sqrt{2r}L) - \sqrt{2r}L \right], \quad (33)$$

while for  $m = 1/2$ , we get

$$\begin{aligned} \langle T_f(L) \rangle &= \frac{1}{r} \left( e^{\sqrt{2r}L} - 1 \right) + \left[ -3\sqrt{2\sqrt{r}} e^{-\sqrt{2r}L} - 3\alpha\sqrt{\pi\sqrt{2}} e^{-\sqrt{2r}L} \left( 1 + \operatorname{erfi}\left(\sqrt{L\sqrt{2r}}\right) \right) \right. \\ &\quad \left. + 3e^{\sqrt{2r}L} \left\{ \sqrt{2\sqrt{r}} + \alpha\sqrt{\pi\sqrt{2}} \left( 1 + \operatorname{erf}\left(\sqrt{L\sqrt{2r}}\right) \right) \right\} - 2r^{\frac{3}{4}}L(3 + 8\alpha\sqrt{L}) \right] \frac{1}{24 \alpha^2 r^{\frac{3}{4}}}. \end{aligned} \quad (34)$$

However, for general values of  $m$ , it is difficult to perform this integration analytically, so we compute it numerically. In Figure 3, we compare our theoretical expression with the same obtained from the numerical simulations for three values of  $m$ . For all cases, we observe an excellent match with the simulation data.

In Eq. (27), we saw that the mean work diverges as  $r \rightarrow 0^+$  for  $m > 1$ , while it approaches zero for  $m < 1$ . It is quite natural to ask how  $\langle T_f(L) \rangle$  behaves for small values of  $r$ . To study this, we separate out the contribution of the trapping potential to  $\langle T_f(L) \rangle$  in Eq. (29) as

$$\langle T(r, L) \rangle_{\text{exe}} = \langle T_f(L) \rangle - \frac{1}{r} \left( e^{\sqrt{2r}L} - 1 \right), \quad (35)$$

$$= \frac{r}{\bar{F}_0(r|0; -L)} \int_{-L}^{\infty} dx \bar{P}_0(x, r; -L) \langle t_f(x; 0) \rangle_R. \quad (36)$$

The subscript ‘exe’ in  $\langle T(r, L) \rangle_{\text{exe}}$  is used to indicate the ‘excess’ time arising due to the non-instantaneous resetting mechanism. Physically  $\langle T(r, L) \rangle_{\text{exe}}$  represents the average time the process spends in its resetting/return phase. For  $r \rightarrow 0^+$  limit, we have shown in Appendix C

$$\langle T(r, L) \rangle_{\text{exe}} \simeq \begin{cases} \frac{L}{\alpha} \frac{\Gamma(3-m)}{(2-m)} (2r)^{\frac{m-1}{2}}, & \text{for } m < 2, \\ \frac{\sqrt{2r}L}{2\alpha} \ln\left(\frac{\alpha}{2r}\right), & \text{for } m = 2, \\ \sqrt{2r}L \left(\frac{m}{2\alpha}\right)^{2/m} \mathbb{C}_m, & \text{for } m > 2, \end{cases} \quad (37)$$

where  $\mathbb{C}_m$  is a  $m$ -dependent constant term defined in Eq. (B.17). Contrary to the mean work, we see that the mean excess time  $\langle T(r, L) \rangle_{\text{exe}}$  diverges as  $\sim r^{-\frac{1-m}{2}}$  for  $m < 1$  in the  $r \rightarrow 0^+$  limit, while it becomes zero for  $m > 1$ . The approach to this zero value depends on the exponent  $m$  as shown in Eq. (37). For the linear case ( $m = 1$ ),  $\langle T(r, L) \rangle_{\text{exe}}$  does not depend on  $r$  and is equal to  $\langle T(r, L) \rangle_{\text{exe}} \simeq L/\alpha$ . This is also consistent with its exact expression in Eq. (33).

Let us understand the scaling relation in Eq. (37) more intuitively. For small  $r$ , the total number of resetting is also small. Let us consider the situation where only one resetting event takes place ( $n = 1$ ). This typically happens after a time  $\tau_1 \sim \gamma$  when the position of the particle is  $x_1 = x(\tau_1) \sim \sqrt{\tau_1}$ , see left panel in Figure 1. We break this trajectory into three parts: (i) diffusive phase for time  $\tau_1$  (ii) resetting phase for time  $t_1$  and (iii) absorbing phase for time  $l$ . In the diffusive phase (i), the particle survives the absorbing wall with a probability  $\text{erf}(L/\sqrt{2\tau_1}) \sim L\sqrt{r}$ . On the other hand, during the resetting phase (ii), the particle makes a first-passage visit to the origin, starting from  $x_1 \sim 1/\sqrt{r}$  in presence of the potential  $U_R(x)$ . Therefore, this segment will contribute  $\langle t_f(x_1; 0) \rangle_R$  to the mean excess time. Since, we are only interested in calculating the total time spend in the resetting phase, the last segment leading to the absorption does not contribute to this (the potential is switched off in this segment). The total contribution for  $n = 1$  can then be written as

$$\langle T(r, L) \rangle_{\text{exe}} \sim L\sqrt{r} \times \langle t_f(x_1; 0) \rangle_R. \quad (38)$$

Recall that  $x_1 \sim 1/\sqrt{r}$  which for  $r \rightarrow 0$  limit takes a large value. Using the asymptotic form of  $\langle t_f(x_1; 0) \rangle_R$  from Eq. (B.20) for different values of  $m$ , one essentially recovers the  $r$ -scaling in Eq. (37). Higher values of  $n$  give sub-leading corrections.

## 6. Trade-off relation for $U_R(x) = \alpha|x|^m/m$

Our study so far has shown that one always incurs a thermodynamic cost while applying an external potential to return the particle to a desired location. A stronger potential rapidly resets the particle, thereby reducing the first-passage time to find the target. However, the cost associated with employing such a stronger potential is quite significant. In contrast, a weaker potential involves lower cost, but the time spent during the return phase is generally higher. In this section, we will minimise the average first-passage time for a given value of the expected work  $\langle W(L) \rangle$ . More specifically, we will

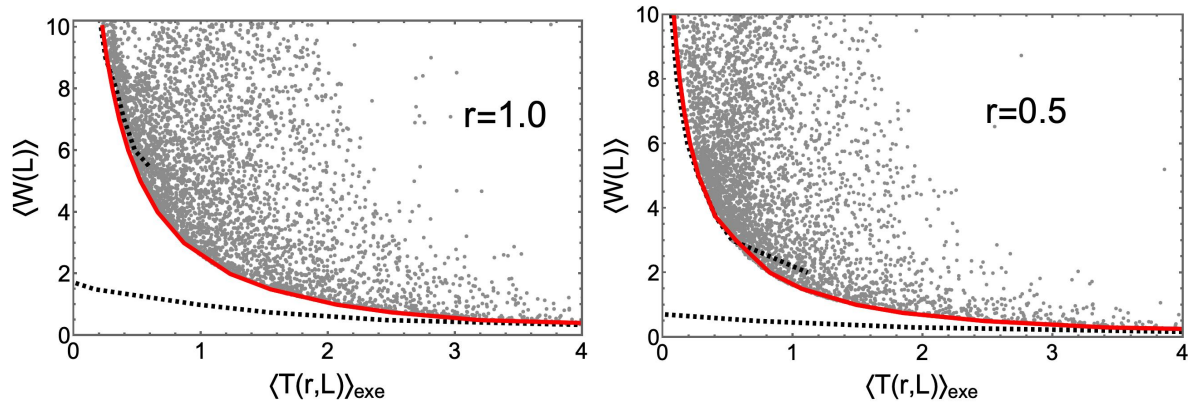


**Figure 4.** Plot of  $\langle W(L) \rangle$  vs  $\langle T(r, L) \rangle_{\text{exe}}$  for  $r = 1$  (left panel) and  $r = 0.5$  (right panel), with  $L = 1$  for both panels. Each gray symbol represents a randomly generated pair of  $m$  and  $\alpha$  values, which are then used in Eqs. (26) and (36) to calculate  $\langle W(L) \rangle$  and  $\langle T(r, L) \rangle_{\text{exe}}$  respectively. The red curve is the Pareto front, obtained by solving Eq. (41) numerically. It is evident that all possible values lie above this curve. In both panels, the black dashed lines represent the asymptotic expressions in Eqs. (42) and (43) for small and large values of the work. To compare the results for  $\langle W(L) \rangle \rightarrow \infty$ , we also need the sub-leading correction in Eq. (43). We set this correction to a constant value: 0.11 for  $r = 1$  and 0.12 for  $r = 0.5$ .

focus on the family of potentials in Eq. (23), and use the results derived for them to obtain the Pareto front.

To understand the cost-time relation, we have plotted  $\langle W(L) \rangle$  and  $\langle T(r, L) \rangle_{\text{exe}}$  in Figure 4 for  $r = 1$  (left panel) and  $r = 0.5$  (right panel). For each  $r$ , gray symbols correspond to the several values of  $m$  and  $\alpha$ . We essentially generate a pair of  $m$  and  $\alpha$  values randomly, which are then used in Eqs. (26) and (36) to obtain  $\langle W(L) \rangle$  and  $\langle T(r, L) \rangle_{\text{exe}}$ . Our plots clearly show that there is a limit on how much  $\langle T(r, L) \rangle_{\text{exe}}$  can be minimised for a given value of work. Once this limit (shown in red) is reached, the expected first-passage time can no longer be minimized further, and to decrease  $\langle T(r, L) \rangle_{\text{exe}}$  beyond this point, one must increase the cost. Different values of work yield different optimal solutions, collectively forming the Pareto front depicted in red in Figure 4.

Let us now calculate the Pareto front. Remember that the resetting potential  $U_R(x)$  is characterised by two parameters,  $\alpha$  and  $m$ . In this analysis, we optimise with respect to the exponent  $m$ , which controls the shape of the potential. Following Eq. (26), the stiffness parameter  $\alpha$  for a given work value is

$$\alpha = \frac{\langle W(L) \rangle}{\mathcal{G}(m, r, L)}, \quad (39)$$

| Expected work $\langle W(L) \rangle$ | $m^*$ for $r = 1$ | $m^*$ for $r = 0.5$ |
|--------------------------------------|-------------------|---------------------|
| 0.1                                  | 3.4               | 3.0                 |
| 0.5                                  | 2.3               | 1.9                 |
| 0.75                                 | 2                 | 1.7                 |
| 1                                    | 1.9               | 1.5                 |
| 2                                    | 1.6               | 1.4                 |
| 3                                    | 1.5               | 1.2                 |
| 4                                    | 1.4               | 1.2                 |

**Table 1.** Optimal potential for  $\langle T(r, L) \rangle_{\text{exe}}$  for a given value of  $\langle W(L) \rangle$ . We have obtained  $m^*$  by numerically solving Eq. (41), for two different values of the resetting rate,  $r = 1$  and  $r = 0.5$  but with the target location fixed to  $L = 1$  for both cases.

with function  $\mathcal{G}(m, r, L)$  defined as

$$\mathcal{G}(m, r, L) = \frac{1}{2m(2r)^{m/2}} \left[ \Gamma(m+1) \left\{ 2 \sinh(\sqrt{2r}L) + e^{\sqrt{2r}L} - (-1)^{-m-1} e^{-\sqrt{2r}L} \right\} \right. \\ \left. + (-1)^{-m-1} e^{-\sqrt{2r}L} \Gamma(m+1, -\sqrt{2r}L) - e^{\sqrt{2r}L} \Gamma(m+1, \sqrt{2r}L) \right]. \quad (40)$$

We insert this expression of  $\alpha$  in Eq. (36) to express  $\langle T(r, L) \rangle_{\text{exe}}$  completely as a function of  $m$  for a given  $\langle W(L) \rangle$ ,  $r$  and  $L$ . Solving for

$$\left. \frac{\partial \langle T(r, L) \rangle_{\text{exe}}}{\partial m} \right|_{m=m^*} = 0, \quad (41)$$

numerically then gives us the optimal potential shape that optimises the  $\langle T(r, L) \rangle_{\text{exe}}$  for a given value of the expected work. We repeat this analysis across several values of  $\langle W(L) \rangle$ , while keeping the values of  $r$  and  $L$  fixed. The associated optimal solutions  $m^*$  are presented in Table 1 as a function of  $\langle W(L) \rangle$  for two different values of the resetting rate. We have plotted the optimal  $\langle W(L) \rangle$  and  $\langle T(r, L) \rangle_{\text{exe}}$  corresponding to  $m = m^*$  in Figure 4 (shown in red). Clearly all other values of averages lie above this red curve for both panels. To sum up, our analysis gives the exact Pareto front for the expected work and the expected first-passage time for a family of potentials  $U_R(x) = \alpha|x|^m/m$ . It shows that for a given cost, there is a fundamental limit on how much the first-passage time can be minimised.

While we have numerically constructed the exact Pareto front, it is desirable to ask if any quantitative formula can be derived. It turns out possible to do heuristic analysis in the asymptotic regimes where  $\langle W(L) \rangle$  is either large or small. From Eq. (39), it then follows that  $\alpha$  is also large or small, and one can then perform a suitable perturbative expansion in  $\alpha$  or  $1/\alpha$ . This yields us simplified relations between the work and first-

passage time. In Appendix D, we demonstrate that the Pareto front takes the form

$$\langle T(r, L) \rangle_{\text{exe}} \simeq \frac{\mathbb{A}_{m^*}(r, L)}{\langle W(L) \rangle^{1/m^*}} - \mathbb{B}_{m^*}(r, L), \quad \text{as } \langle W(L) \rangle \rightarrow 0, \quad (42)$$

$$\simeq \frac{\mathbb{Y}_{m^*}(r, L)}{\langle W(L) \rangle}, \quad \text{as } \langle W(L) \rangle \rightarrow \infty, \quad (43)$$

with  $\mathbb{A}_{m^*}(r, L)$ ,  $\mathbb{B}_{m^*}(r, L)$  and  $\mathbb{Y}_{m^*}(r, L)$  defined in Eqs. (D.3), (D.4) and (D.7) respectively. Moreover, the optimal  $m^*$  is given in Table 1. We have plotted these asymptotic results in Figure 4 (indicated by black dashed lines) along with their exact counterpart. We see that Eqs. (42) and (43) essentially converge with the exact result in the appropriate regimes. For comparison of  $\langle W(L) \rangle \rightarrow \infty$ , we also need the sub-leading correction in Eq. (43), which our heuristic analysis cannot account for and a further study is required. In our study, we set this correction to a constant value: 0.11 for  $r = 1$  and 0.12 for  $r = 0.5$ .

## 7. Conclusion

In this paper, we presented an exact thermodynamic analysis of a diffusing particle with stochastic return. Our approach gives the renewal formula for the joint distribution of the work done and the first-passage time. Compared to some earlier works [63], we were able to derive general expressions for the averages of these quantities for arbitrary confining potentials. This has, for the first time, allowed us to carry out optimisation problem with respect to the shape of the potential. In particular, for a family of potentials  $U_R(x) = \alpha|x|^m/m$ , we have optimised the expected first-passage time keeping the value of average work fixed. Our work shows for a given thermodynamic cost, there is a fundamental limit on how much the first-passage time can be minimised. Using the optimal solutions for different values of the work, we have obtained the exact Pareto front, and used it to demonstrate a trade-off relation between the first-passage time and the work done. As a side product, our analysis also establishes a thermodynamic connection of some non-thermodynamic cost functions studied in the resetting literature [68, 69].

A crucial assumption throughout our work is that the first-passage event  $T_f$  is achieved only during the diffusive phase, and not during the return phase. A promising future direction is to relax this assumption, and study its effect on the cost-time trade-off relation. It might be possible to extend our method to include this scenario and will be pursued elsewhere. It should also be possible to generalise our framework to higher dimensional settings as well as to other Markov processes. Finally, it would be interesting to compare our general expressions on expected first-passage time and work with resetting experiments [31–33].



## Acknowledgement

The author acknowledges the support of Novo Nordisk Foundation under the grant number NNF21OC0071284, for funding their postdoctoral position.

## Appendix A. $\langle W(L) \rangle$ as $r \rightarrow 0^+$

In Eq. (27), we saw that for small values of  $r$ , the mean work diverges as  $r^{(1-m)/2}$  for  $m > 1$  whereas it converges to zero for  $m < 1$ . For  $m = 1$ , it possesses a non-zero value independent of the resetting rate  $r$ . To derive this, we first recall that for small  $r$ , the particle will experience only a small number of resets. Therefore, the joint distribution  $\mathcal{P}(W, T_f)$  in Eq. (17) will have leading contributions from those  $\mathcal{C}_n$  with small  $n$ . Let us take the first two leading contributions

$$\mathcal{P}(W, T_f) \simeq \mathcal{C}_0 + \mathcal{C}_1, \quad (\text{A.1})$$

with  $\mathcal{C}_1$  and  $\mathcal{C}_0$  given in Eqs. (14) and (16) respectively. Integrating out the first-passage time gives us the marginal distribution  $\mathcal{P}_w(W) = \int_0^\infty dT_f \mathcal{P}(W, T_f)$  as

$$\mathcal{P}_w(W) \simeq \bar{F}_0(r | 0; -L) \delta(W) + r \bar{F}_0(r | 0; -L) \int_{-L}^\infty dx \delta(W - U_R(x)) \bar{P}_0(x, r; -L).$$

We use this expression to calculate the approximate form of the mean as

$$\langle W(L) \rangle \simeq r \bar{F}_0(r | 0; -L) \int_{-L}^\infty dx U_R(x) \bar{P}_0(x, r; -L), \quad (\text{A.2})$$

$$\simeq \frac{\sqrt{r}\alpha}{\sqrt{2}m} \int_{-L}^\infty dx |x|^m \left[ e^{-\sqrt{2r}|x|} - e^{-\sqrt{2r}(x+2L)} \right]. \quad (\text{A.3})$$

In writing the second line, we have used  $\bar{F}_0(r \rightarrow 0 | 0; -L) \simeq 1$  from Eq. (24) and used Eq. (25) to replace  $\bar{P}_0(x, r; -L)$ . We have also plugged  $U_R(x) = \alpha|x|^m/m$ . We now perform a transformation  $y = \sqrt{2r}x$  in Eq (A.3) and recast it as

$$\langle W(L) \rangle \simeq \frac{\alpha}{2m} \frac{\alpha}{(2r)^{m/2}} \int_0^\infty dy y^m \left[ e^{-y} - e^{-(y+2\sqrt{2r}L)} \right], \quad (\text{A.4})$$

$$\simeq \frac{\alpha}{2m} \frac{\alpha}{(2r)^{m/2}} e^{-2\sqrt{2r}L} \left( e^{2\sqrt{2r}L} - 1 \right) \Gamma(m+1). \quad (\text{A.5})$$

Expanding further for small  $r$  gives

$$\langle W(L) \rangle \simeq \frac{\alpha L \Gamma(m+1)}{m} (2r)^{\frac{1-m}{2}} \quad \text{as } r \rightarrow 0^+. \quad (\text{A.6})$$

We have quoted this result in Eq. (27) in the main text.

## Appendix B. Mean first-passage time for a diffusing particle in general potential

In this appendix, we will consider a particle diffusing in one dimension in presence of a general confining potential  $U_R(x)$  and calculate the mean first-passage time to reach a target location  $x_T$  starting from some position  $x_0$ . We denote this by  $\langle t_f(x_0; x_T) \rangle_R$  and assume  $x_0 \geq x_T$ . Our starting point is write the backward Fokker-Planck equation for the survival probability  $Q_R(t|x_0; x_T)$  as [71]

$$\frac{\partial Q_R(t|x_0; x_T)}{\partial t} = \frac{1}{2} \frac{\partial^2 Q_R(t|x_0; x_T)}{\partial x_0^2} - U'_R(x_0) \frac{\partial Q_R(t|x_0; x_T)}{\partial x_0}, \quad (\text{B.1})$$

with the initial condition  $Q_R(0|x_0; x_T) = 1$  and the boundary conditions  $Q_R(t|x_0 = x_T; x_T) = 0$  and  $Q_R(0|x_0 \rightarrow \infty; x_T) = 1$ . Taking Laplace transformation with respect to  $t$  ( $\rightarrow s$ ), Eq. (B.1) becomes

$$\frac{1}{2} \frac{\partial^2 \bar{Q}_R(s|x_0; x_T)}{\partial x_0^2} - U'_R(x_0) \frac{\partial \bar{Q}_R(s|x_0; x_T)}{\partial x_0} - s \bar{Q}_R(s|x_0; x_T) = -1, \quad (\text{B.2})$$

with  $\bar{Q}_R(s|x_0; x_T)$  denoting the Laplace transformation of the survival probability. We next use the relation between the first-passage time distribution and the survival probability,  $F_R(t|x_0; x_T) = -\partial_t Q_R(t|x_0; x_T)$  and obtain

$$\langle t_f(x_0; x_T) \rangle_R = \int_0^\infty dt t F_R(t|x_0; x_T) = \bar{Q}_R(s=0|x_0; x_T). \quad (\text{B.3})$$

Therefore putting  $s = 0$  in Eq. (B.2), we obtain a second-order differential equation for the mean as

$$\frac{1}{2} \frac{\partial^2 \langle t_f(x_0; x_T) \rangle_R}{\partial x_0^2} - U'_R(x_0) \frac{\partial \langle t_f(x_0; x_T) \rangle_R}{\partial x_0} = -1. \quad (\text{B.4})$$

Multiplying both sides by  $2e^{-2U_R(x_0)}$ , it can be rewritten as

$$\frac{\partial}{\partial x_0} \left[ e^{-2U_R(x_0)} \frac{\partial \langle t_f(x_0; x_T) \rangle_R}{\partial x_0} \right] = -2e^{-2U_R(x_0)}. \quad (\text{B.5})$$

Using the boundary condition  $e^{-2U_R(x_0)} \frac{\partial \langle t_f(x_0; x_T) \rangle_R}{\partial x_0} \Big|_{x_0 \rightarrow \infty} = 0$ , one can integrate the above equation as

$$\frac{\partial \langle t_f(x_0; x_T) \rangle_R}{\partial x_0} = 2e^{2U_R(x_0)} \int_{x_0}^\infty dz e^{-2U_R(z)}. \quad (\text{B.6})$$

Again integrating this equation from  $x_T$  to  $x_0$  and using the boundary condition  $\langle t_f(x_T; x_T) \rangle_R = 0$ , since the first-passage time to  $x_T$ , starting from the same position  $x_0 = x_T$  is always zero, one obtains

$$\langle t_f(x_0; x_T) \rangle_R = 2 \int_{x_T}^{x_0} dy e^{2U_R(y)} \int_y^\infty dz e^{-2U_R(z)}. \quad (\text{B.7})$$

Remember that we have assumed  $x_0 \geq x_T$  in order to derive this expression. For the opposite case  $x_0 < x_T$ , the same derivation gives

$$\langle t_f(x_0; x_T) \rangle_R = 2 \int_{x_0}^{x_T} dy e^{2U_R(y)} \int_{-\infty}^y dz e^{-2U_R(z)}. \quad (\text{B.8})$$

Combining these two results and setting the target to the origin,  $x_T = 0$ , it follows

$$\langle t_f(x_0; 0) \rangle_R = \begin{cases} 2 \int_0^{x_0} dy e^{2U_R(y)} \int_y^{\infty} dz e^{-2U_R(z)}, & \text{if } x_0 \geq 0, \\ 2 \int_{x_0}^0 dy e^{2U_R(y)} \int_{-\infty}^y dz e^{-2U_R(z)}, & \text{if } x_0 < 0. \end{cases} \quad (\text{B.9})$$

We have quoted this expression in Eq. (31).

### Appendix B.1. Resetting potential $U_R(x) = \alpha|x|^m/m$

For a family of potentials  $U_R(x) = \alpha|x|^m/m$  with  $m > 0$ , one can carry out the integrations in Eq. (B.9) and obtain a closed-form expression for the mean first-passage time. To achieve this, let us focus on  $x_0 > 0$  and rewrite Eq. (B.7) as

$$\langle t_f(x_0; 0) \rangle_R = 2 \int_0^{x_0} dy e^{\frac{2\alpha y^m}{m}} \int_y^{\infty} dz e^{-\frac{2\alpha z^m}{m}}. \quad (\text{B.10})$$

The integration over  $z$  can be explicitly performed as

$$\begin{aligned} \int_y^{\infty} dz e^{-\frac{2\alpha z^m}{m}} &= \frac{1}{m} \left( \frac{m}{2\alpha} \right)^{\frac{1}{m}} \Gamma \left( \frac{1}{m}, \frac{2\alpha y^m}{m} \right), \\ &= \frac{1}{m} \left( \frac{m}{2\alpha} \right)^{\frac{1}{m}} \left[ \Gamma \left( \frac{1}{m} \right) - e^{-\frac{2\alpha y^m}{m}} \sum_{q=0}^{\infty} \frac{\Gamma \left( \frac{1}{m} \right)}{\Gamma \left( \frac{1}{m} + q + 1 \right)} \left( \frac{2\alpha y^m}{m} \right)^{\frac{1}{m} + q} \right]. \end{aligned}$$

In going to the second line, we have used the series representation of the upper Gamma function [72]

$$\Gamma(n, x) = \Gamma(n) - e^{-x} \sum_{q=0}^{\infty} \frac{\Gamma(n)}{\Gamma(n + q + 1)} x^{n+q}. \quad (\text{B.11})$$

Plugging the above expression in Eq. (B.10) gives

$$\langle t_f(x_0; 0) \rangle_R = \frac{2}{m} \left( \frac{m}{2\alpha} \right)^{\frac{1}{m}} \left[ \Gamma \left( \frac{1}{m} \right) \int_0^{x_0} dy e^{\frac{2\alpha y^m}{m}} - \sum_{q=0}^{\infty} \frac{\Gamma \left( \frac{1}{m} \right)}{\Gamma \left( \frac{1}{m} + q + 1 \right)} \left( \frac{2\alpha}{m} \right)^{\frac{1}{m} + q} \frac{x_0^{mq+2}}{mq+2} \right]. \quad (\text{B.12})$$

Once again the integration over  $y$  can be analytically carried out in terms of the Gamma functions. On the other hand, the other term containing summation over  $q$

can be simplified using Mathematica in terms of the hypergeometric functions. The resulting expression reads

$$\begin{aligned} \langle t_f(x_0; 0) \rangle_R &= \frac{2}{m} \left( \frac{m}{2\alpha} \right)^{\frac{1}{m}} \left[ \frac{(-1)^{-\frac{1}{m}}}{m} \left( \frac{m}{2\alpha} \right)^{\frac{1}{m}} \Gamma\left(\frac{1}{m}\right) \left\{ \Gamma\left(\frac{1}{m}\right) - \Gamma\left(\frac{1}{m}, -\frac{2\alpha}{m} x_0^m\right) \right\} \right. \\ &\quad \left. - \frac{m x_0}{2} \left( \frac{2\alpha x_0^m}{m} \right)^{\frac{1}{m}} {}_2F_2\left(\left\{1, \frac{2}{m}\right\}, \left\{1 + \frac{1}{m}, 1 + \frac{2}{m}\right\}; \frac{2\alpha}{m} x_0^m\right) \right]. \end{aligned} \quad (\text{B.13})$$

*Appendix B.2.  $\langle t_f(x_0; 0) \rangle_R$  for large  $x_0$*

For subsequent sections, it is useful to simplify the expression of the mean first-passage time for larger values of  $x_0$ . To achieve this, we will use the following expansions of the Gamma function and generalised hypergeometric function:

$$\Gamma\left(\frac{1}{m}, -y\right) = \frac{(-1)^{1+\frac{1}{m}} e^y}{y^{1-\frac{1}{m}}} \left[ 1 + \sum_{q=1}^{\infty} \frac{(m-1)(2m-1)\dots(qm-1)}{(my)^q} \right], \quad (\text{B.14})$$

$$\begin{aligned} {}_2F_2\left(\left\{1, \frac{2}{m}\right\}, \left\{1 + \frac{1}{m}, 1 + \frac{2}{m}\right\}; y\right) &\simeq \frac{2\Gamma\left(\frac{1}{m}\right) e^y}{m^2 y^{1+\frac{1}{m}}} \left[ 1 + \sum_{q=1}^{\infty} \frac{(m-1)(2m-1)\dots(qm-1)}{(my)^q} \right] \\ &+ \frac{2\Gamma\left(1 - \frac{2}{m}\right) \Gamma\left(\frac{1}{m}\right) \Gamma\left(\frac{2}{m}\right)}{m^2 (-1)^{\frac{2}{m}} \Gamma\left(1 - \frac{1}{m}\right) y^{\frac{2}{m}}} + \frac{2}{(m-2)my} - \frac{1}{m^2 y^2} + \dots \end{aligned} \quad (\text{B.15})$$

The second expansion is valid for all values of  $m$  except  $m = 1, 2$ . We will consider these two special cases later, and for now proceed with  $m \neq 1, 2$ . Substituting them in Eq. (B.13), we obtain for large  $x_0$

$$\langle t_f(x_0; 0) \rangle_R \simeq \left( \frac{m}{2\alpha} \right)^{\frac{2}{m}} \left[ \mathbb{C}_m + \frac{2 x_0^{2-m}}{m(2-m)} \left( \frac{2\alpha}{m} \right)^{\frac{2}{m}-1} + \frac{x_0^{2-2m}}{m^2} \left( \frac{2\alpha}{m} \right)^{\frac{2}{m}-2} \right], \quad (\text{B.16})$$

$$\text{with } \mathbb{C}_m = \frac{2 \Gamma\left(\frac{1}{m}\right)^2}{(-1)^{\frac{1}{m}} m^2} - \frac{2 \Gamma\left(1 - \frac{2}{m}\right) \Gamma\left(\frac{1}{m}\right) \Gamma\left(\frac{2}{m}\right)}{(-1)^{\frac{2}{m}} m^2 \Gamma\left(1 - \frac{1}{m}\right)}. \quad (\text{B.17})$$

For  $m < 2$ , the second term in Eq. (B.16) diverges for  $x_0 \rightarrow \infty$  while the first term is just a constant. Therefore, the mean first-passage time also diverges as  $\langle t_f(x_0; 0) \rangle_R \sim x_0^{2-m}$  for  $m < 2$ . However, if  $m > 2$ , the second terms rather decays with  $x_0$  and the first term then gives the leading order contribution. Thus,  $\langle t_f(x_0; 0) \rangle_R$  attains a  $x_0$ -independent value for  $m > 2$  as  $x_0$  becomes large. For the marginal case of  $m = 2$ , we replace  $m = (2 - \epsilon)$  in Eq. (B.16) and then take  $\epsilon \rightarrow 0^+$  limit. This leads to a logarithmic behaviour of the form

$$\langle t_f(x_0; 0) \rangle_R \simeq \frac{1}{\alpha} \left[ \frac{\gamma_E + \ln 4}{2} + \frac{1}{2} \ln(\alpha x_0^2) \right], \quad (\text{for } m = 2), \quad (\text{B.18})$$

for large  $x_0$ . Here  $\gamma_E$  is the Euler–Mascheroni constant. Finally, for the linear potential case  $m = 1$ , it follows directly from Eq. (B.13) that

$$\langle t_f(x_0; 0) \rangle_R = \frac{x_0}{\alpha}, \quad (\text{B.19})$$

for all values of  $x_0$ . Combining results for all  $m$ , one can write

$$\langle t_f(x_0; 0) \rangle_R \simeq \begin{cases} x_0^{2-m}/(2-m)\alpha, & \text{for } m < 2, \\ \ln(\alpha x_0^2)/2\alpha, & \text{for } m = 2, \\ \mathbb{C}_m(m/2\alpha)^{\frac{2}{m}}, & \text{for } m > 2. \end{cases} \quad (\text{B.20})$$

### Appendix C. $\langle T(r, L) \rangle_{\text{exe}}$ as $r \rightarrow 0^+$

In Eq. (37), we quoted the excess time  $\langle T(r, L) \rangle_{\text{exe}}$  in the limit  $r \rightarrow 0^+$  and found it to crucially depend on the exponent  $m$ . Here, we will present a derivation of this result. Let us begin with its definition in Eq. (36)

$$\langle T(r, L) \rangle_{\text{exe}} = \frac{r}{\bar{F}_0(r|0; -L)} \int_{-L}^{\infty} dx \bar{P}_0(x, r; -L) \langle t_f(x; 0) \rangle_R, \quad (\text{C.1})$$

$$= \frac{\sqrt{r} e^{\sqrt{2r}L}}{\sqrt{2}} \int_{-L}^{\infty} dx \left[ e^{-\sqrt{2r}|x|} - e^{-\sqrt{2r}(x+2L)} \right] \langle t_f(x; 0) \rangle_R, \quad (\text{C.2})$$

where in the second line, we have plugged  $\bar{F}_0(r|0; -L)$  and  $\bar{P}_0(x, r; -L)$  from Eqs. (24) and (25) respectively. We next perform a change of variable  $x = y/\sqrt{2r}$  and recast the integration as

$$\langle T(r, L) \rangle_{\text{exe}} = \frac{e^{\sqrt{2r}L}}{2} \int_{-\sqrt{2r}L}^{\infty} dy \left[ e^{-|y|} - e^{-(y+2\sqrt{2r}L)} \right] \langle t_f(y/\sqrt{2r}; 0) \rangle_R. \quad (\text{C.3})$$

For small  $r$ , the argument of  $\langle t_f(y/\sqrt{2r}; 0) \rangle_R$  becomes large, and this allows us to use the asymptotic expressions of  $\langle t_f(y/\sqrt{2r}; 0) \rangle_R$  derived in Appendix B.2.

#### Appendix C.1. Case $m = 2$

For example for  $m = 2$ , we utilize the result in Eq. (B.18) and obtain

$$\langle T(r, L) \rangle_{\text{exe}} \simeq \frac{e^{\sqrt{2r}L}}{2\alpha} \left[ \left( \frac{\gamma_E + \ln 4 + \ln(\alpha/2r)}{2} \right) \int_{-\sqrt{2r}L}^{\infty} dy \left( e^{-|y|} - e^{-(y+2\sqrt{2r}L)} \right) + \int_{-\sqrt{2r}L}^{\infty} dy \ln |y| \left( e^{-|y|} - e^{-(y+2\sqrt{2r}L)} \right) \right]. \quad (\text{C.4})$$

The integrations appearing in this expression can be carried out analytically

$$\int_{-a}^{\infty} dy \left( e^{-|y|} - e^{-(y+2a)} \right) = 2(1 - e^{-a}), \quad (\text{C.5})$$

$$\int_{-a}^{\infty} dy \ln |y| \left( e^{-|y|} - e^{-(y+2a)} \right) = e^{-2a} [\text{Chi}(a) + \text{Shi}(a) - 2\gamma_E - \Gamma(0, a) - 2e^{-a} \ln a], \quad (\text{C.6})$$

where  $\text{Chi}(a)$  and  $\text{Shi}(a)$  are the hyperbolic cosine and sine integrals respectively. Plugging them in Eq. (C.4) and then taking  $r \rightarrow 0$  limit, we obtain

$$\langle T(r, L) \rangle_{\text{exe}} \simeq \frac{\sqrt{2r}L}{2\alpha} [\ln 4 - \gamma_E + \ln(\alpha/2r)], \quad \text{for } m = 2. \quad (\text{C.7})$$

### Appendix C.2. Case $m < 2$

For  $m < 2$ , we will substitute  $\langle t_f(y/\sqrt{2r}; 0) \rangle_R$  from Eq. (B.20) in Eq. (C.3) and perform the integration over  $y$  to yield

$$\begin{aligned} \langle T(r, L) \rangle_{\text{exe}} \simeq & \frac{(2r)^{\frac{m-2}{2}}}{2\alpha(2-m)} \left[ \Gamma(3-m) - \Gamma\left(3-m, \sqrt{2r}L\right) + 2e^{-\sqrt{2r}L} \Gamma(3-m) \sinh\left(\sqrt{2r}L\right) \right. \\ & \left. + (-1)^m e^{-2\sqrt{2r}L} \left\{ \Gamma(3-m) - \Gamma\left(3-m, -\sqrt{2r}L\right) \right\} \right]. \end{aligned} \quad (\text{C.8})$$

For small  $r$ , we use the series expansion

$$\Gamma(3-m) - \Gamma(3-m, \sqrt{2r}L) \simeq \frac{(\sqrt{2r}L)^{3-m}}{(3-m)} + \frac{(\sqrt{2r}L)^{4-m}}{(m-4)}, \quad (\text{C.9})$$

which then gives us the simplified expression

$$\langle T(r, L) \rangle_{\text{exe}} \simeq \frac{L \Gamma(3-m)}{\alpha(2-m)} (2r)^{\frac{m-1}{2}}, \quad \text{for } m < 2. \quad (\text{C.10})$$

### Appendix C.3. Case $m > 2$

Once again, we use the approximate expression of  $\langle t_f(y/\sqrt{2r}; 0) \rangle_R$  from Eq. (B.20) and obtain

$$\langle T(r, L) \rangle_{\text{exe}} \simeq \mathbb{C}_m (m/2\alpha)^{2/m} \left(1 - e^{-\sqrt{2r}L}\right) \simeq \mathbb{C}_m (m/2\alpha)^{2/m} \sqrt{2r}L. \quad (\text{C.11})$$

## Appendix D. Calculation of the Pareto front

In this appendix, we will derive simplified expressions for the Pareto front in the limits of large and small values of the expected work  $\langle W(L) \rangle$ . Let us first look at the  $\langle W(L) \rangle \rightarrow 0$  limit. Eq. (39) then dictates that the potential strength  $\alpha$  is also small, allowing for a perturbation analysis in  $\alpha$ . Following Eq. (B.12), we then obtain

$$\langle t_f(x; 0) \rangle_R = \frac{2|x| \Gamma\left(\frac{1}{m}\right)}{m} \left(\frac{m}{2\alpha}\right)^{\frac{1}{m}} - x^2. \quad (\text{D.1})$$

We have assumed  $m > 1$  here, since Table (1) shows that the optimal  $m$  for small  $\langle W(L) \rangle$  is always greater than 1. Plugging this in the definition of the excess time in Eq. (36) yields

$$\langle T(r, L) \rangle_{\text{exe}} \simeq \frac{\mathbb{A}_m(r, L)}{\langle W(L) \rangle^{1/m}} - \mathbb{B}_m(r, L), \quad (\text{D.2})$$

where the two function  $\mathbb{A}_m(r, L)$  and  $\mathbb{B}_m(r, L)$  are given by

$$\mathbb{A}_m(r, L) = \sqrt{\frac{2}{r}} \left( \frac{m \mathcal{G}(m, r, L)}{2} \right)^{\frac{1}{m}} \Gamma\left(\frac{1}{m} + 1\right) \left\{ 2 \sinh(\sqrt{2r}L) - \sqrt{2r}L \right\}, \quad (\text{D.3})$$

$$\mathbb{B}_m(r, L) = \frac{1}{r} \left( e^{\sqrt{2r}L} - 1 - r^2 L \right), \quad (\text{D.4})$$

with  $\mathcal{G}(m, r, L)$  defined in Eq. (40). In order to construct Pareto front, we simply put  $m = m^*$  in Eq. (D.2) with values of  $m^*$  taken from Table (1).

In the opposite limit of large  $\alpha$ , we use the asymptotic expression of  $\langle t_f(x; 0) \rangle$  in Eq. (B.20) for  $m < 2$

$$\langle t_f(x; 0) \rangle_R \simeq \frac{|x|^{2-m}}{(2-m)\alpha}. \quad (\text{D.5})$$

Here again, we have chosen the expression for  $m < 2$  because the optimal  $m^*$  in Table (1) satisfies this condition for large  $\langle W(L) \rangle$ . Using this expression in Eq. (36) gives us

$$\langle T(r, L) \rangle_{\text{exe}} \simeq \frac{\mathbb{Y}_m(r, L)}{\langle W(L) \rangle}, \quad (\text{D.6})$$

with  $\mathbb{Y}_m(r, L)$  given by

$$\begin{aligned} \mathbb{Y}_m(r, L) = & \frac{e^{\sqrt{2r}L} \mathcal{G}(m, r, L)}{2(2-m)(\sqrt{2r})^{2-m}} \left[ \Gamma(3-m) - \Gamma\left(3-m, \sqrt{2r}L\right) + 2e^{-\sqrt{2r}L} \Gamma(3-m) \sinh\left(\sqrt{2r}L\right) \right. \\ & \left. + (-1)^m e^{-2\sqrt{2r}L} \left\{ \Gamma(3-m) - \Gamma\left(3-m, -\sqrt{2r}L\right) \right\} \right]. \quad (\text{D.7}) \end{aligned}$$

We use the optimal  $m^*$  from Table (1) in Eq. (D.6) to obtain the Pareto front.

## References

- [1] Evans M R and Majumdar S N 2011 *Phys. Rev. Lett.* **106**(16) 160601
- [2] Evans M R and Majumdar S N 2011 *Journal of Physics A: Mathematical and Theoretical* **44** 435001
- [3] Pal A 2015 *Phys. Rev. E* **91**(1) 012113
- [4] Pal A and Reuveni S 2017 *Phys. Rev. Lett.* **118**(3) 030603
- [5] Majumdar S N, Sabhapandit S and Schehr G 2015 *Phys. Rev. E* **91**(5) 052131
- [6] Kusmierz L, Majumdar S N, Sabhapandit S and Schehr G 2014 *Phys. Rev. Lett.* **113**(22) 220602
- [7] Bressloff P C 2020 *Journal of Physics A: Mathematical and Theoretical* **53** 105001
- [8] Reuveni S 2016 *Phys. Rev. Lett.* **116**(17) 170601
- [9] Gupta D 2019 *Journal of Statistical Mechanics: Theory and Experiment* **2019** 033212
- [10] Singh P 2020 *Journal of Physics A: Mathematical and Theoretical* **53** 405005
- [11] Evans M R and Majumdar S N 2018 *Journal of Physics A: Mathematical and Theoretical* **51** 475003
- [12] Kumar V, Sadekar O and Basu U 2020 *Phys. Rev. E* **102**(5) 052129
- [13] Singh P and Pal A 2021 *Phys. Rev. E* **103**(5) 052119
- [14] Stojkoski V, Sandev T, Kocarev L and Pal A 2022 *Journal of Physics A: Mathematical and Theoretical* **55** 104003
- [15] Majumdar S N and Oshanin G 2018 *Journal of Physics A: Mathematical and Theoretical* **51** 435001
- [16] Singh P and Pal A 2022 *Journal of Physics A: Mathematical and Theoretical* **55** 234001
- [17] De Bruyne B and Mori F 2023 *Phys. Rev. Res.* **5**(1) 013122
- [18] Reuveni S, Urbakh M and Klafter J 2014 *Proceedings of the National Academy of Sciences* **111** 4391–4396
- [19] Roldán E, Lisica A, Sánchez-Taltavull D and Grill S W 2016 *Phys. Rev. E* **93**(6) 062411
- [20] Bressloff P C 2020 *Journal of Physics A: Mathematical and Theoretical* **53** 355001

- [21] Pal A, Reuveni S and Rahav S 2021 *Phys. Rev. Res.* **3**(3) L032034
- [22] Stojkoski V, Jolakoski P, Pal A, Sandev T, Kocarev L and Metzler R 2022 *Philosophical Transactions of the Royal Society A: Mathematical, Physical and Engineering Sciences* **380** 20210157
- [23] Santra I 2022 *Europhysics Letters* **137** 52001
- [24] Luby M, Sinclair A and Zuckerman D 1993 *Information Processing Letters* **47** 173–180
- [25] Hamlin P, Thrasher W J, Keyrouz W and Mascagni M 2019 *Monte Carlo Methods and Applications* **25** 329–340
- [26] Evans M R, Majumdar S N and Schehr G 2020 *Journal of Physics A: Mathematical and Theoretical* **53** 193001
- [27] Gupta S and Jayannavar A M 2022 *Frontiers in Physics* **10**
- [28] Nagar A and Gupta S 2023 *Journal of Physics A: Mathematical and Theoretical* **56** 283001
- [29] Pal A, Stojkoski V and Sandev T 2023 Random resetting in search problems arXiv:2310.12057
- [30] Pal A, Kostinski S and Reuveni S 2022 *Journal of Physics A: Mathematical and Theoretical* **55** 021001
- [31] Tal-Friedman O, Pal A, Sekhon A, Reuveni S and Roichman Y 2020 *The Journal of Physical Chemistry Letters* **11** 7350–7355
- [32] Besga B, Bovon A, Petrosyan A, Majumdar S N and Ciliberto S 2020 *Phys. Rev. Res.* **2**(3) 032029
- [33] Besga B, Faisant F, Petrosyan A, Ciliberto S and Majumdar S N 2021 *Phys. Rev. E* **104**(1) L012102
- [34] Pal A, Kuśmierz L and Reuveni S 2020 *Phys. Rev. Res.* **2**(4) 043174
- [35] Pal A, Kuśmierz L and Reuveni S 2019 *New Journal of Physics* **21** 113024
- [36] Pal A, Kuśmierz L and Reuveni S 2019 *Phys. Rev. E* **100**(4) 040101
- [37] Bodrova A S and Sokolov I M 2020 *Phys. Rev. E* **101**(5) 052130
- [38] Masó-Puigdellosas A, Campos D and Méndez V m c 2019 *Phys. Rev. E* **100**(4) 042104
- [39] Tucci G, Gambassi A, Majumdar S N and Schehr G 2022 *Phys. Rev. E* **106**(4) 044127
- [40] Evans M R and Majumdar S N 2018 *Journal of Physics A: Mathematical and Theoretical* **52** 01LT01
- [41] Masó-Puigdellosas A, Campos D and Méndez V 2019 *Journal of Statistical Mechanics: Theory and Experiment* **2019** 033201
- [42] García-Valladares G, Gupta D, Prados A and Plata C A 2024 *Physica Scripta* **99** 045234
- [43] Radice M 2021 *Phys. Rev. E* **104**(4) 044126
- [44] Radice M 2022 *Journal of Physics A: Mathematical and Theoretical* **55** 224002
- [45] Mercado-Vásquez G, Boyer D, Majumdar S N and Schehr G 2020 *Journal of Statistical Mechanics: Theory and Experiment* **2020** 113203
- [46] Santra I, Das S and Nath S K 2021 *Journal of Physics A: Mathematical and Theoretical* **54** 334001
- [47] Gupta D, Plata C A, Kundu A and Pal A 2020 *Journal of Physics A: Mathematical and Theoretical* **54** 025003
- [48] Gupta D, Pal A and Kundu A 2021 *Journal of Statistical Mechanics: Theory and Experiment* **2021** 043202
- [49] Biswas A, Kundu A and Pal A 2023 ArXiv:2307.16294
- [50] Biswas A, Dubey A, Kundu A and Pal A 2024 ArXiv:2406.08975
- [51] Gupta D and Plata C A 2022 *New Journal of Physics* **24** 113034
- [52] Fuchs J, Goldt S and Seifert U 2016 *Europhysics Letters* **113** 60009
- [53] Gupta D, Plata C A and Pal A 2020 *Phys. Rev. Lett.* **124**(11) 110608
- [54] Busiello D M, Gupta D and Maritan A 2020 *Phys. Rev. Res.* **2**(2) 023011
- [55] Pal A and Rahav S 2017 *Phys. Rev. E* **96**(6) 062135
- [56] Pal A, Reuveni S and Rahav S 2021 *Phys. Rev. Res.* **3**(1) 013273
- [57] Pal A, Reuveni S and Rahav S 2021 *Phys. Rev. Res.* **3**(3) L032034
- [58] Alston H, Cocconi L and Bertrand T 2022 *Journal of Physics A: Mathematical and Theoretical* **55** 274004



- [59] Gupta D and Busiello D M 2020 *Phys. Rev. E* **102**(6) 062121
- [60] Olsen K S, Gupta D, Mori F and Krishnamurthy S 2023 ArXiv:2310.11267
- [61] Olsen K S and Gupta D 2024 *Journal of Physics A: Mathematical and Theoretical* **57** 245001
- [62] Mori F, Olsen K S and Krishnamurthy S 2023 *Phys. Rev. Res.* **5**(2) 023103
- [63] Pal P S, Pal A, Park H and Lee J S 2023 *Phys. Rev. E* **108**(4) 044117
- [64] Lahiri S and Gupta S 2024 *Phys. Rev. E* **109**(1) 014129
- [65] Seifert U 2012 *Reports on Progress in Physics* **75** 126001
- [66] Sekimoto K 1998 *Progress of Theoretical Physics Supplement* **130** 17–27
- [67] Ishizaka A and Nemery P 2013 *Multi-criteria Decision Analysis: Methods And Software* (John Wiley and Sons)
- [68] Sunil J C, Blythe R A, Evans M R and Majumdar S N 2023 *Journal of Physics A: Mathematical and Theoretical* **56** 395001
- [69] Sunil J C, Blythe R A, Evans M R and Majumdar S N 2024 ArXiv:2404.00215
- [70] Redner S 2001 *A Guide to First-Passage Processes* (Cambridge University Press)
- [71] Majumdar S N 2005 *Current Science* **89** 93–129
- [72] Olver F W J, Daalhuis A B O, Lozier D W, Schneider B I, Boisvert R F, Clark C W, Miller B R, Saunders B V, Cohl H S and McClain M A NIST Digital Library of Mathematical Functions